

# Unsupervised Rib Delineation in Chest Radiographs by an Integrative Approach

B. Buket Oğul<sup>1</sup>, Emre Sümer<sup>2</sup> and Hasan Oğul<sup>2</sup>

<sup>1</sup>*Akgun Software Company, Ankara, Turkey*

<sup>2</sup>*Department of Computer Engineering, Baskent University, Ankara, Turkey*

**Keywords:** Computer Aided Diagnosis, X-ray Imaging, Medical Image Analysis.

**Abstract:** We address the problem of segmenting ribs in a chest radiography image as an intermediate step for eliminating rib shadows for an effective Computer-Aided Diagnosis System (CAD). To this end, we introduce a complete framework that takes an unprocessed x-ray image and reports the entire rib regions. The system offers a novel strategy to fit a parabola curve to all rib seeds obtained through a log Gabor filtering approach and extend the center curve by a problem-specific region growing technique to delineate the entire rib, which does not necessarily follow a general parabolic model of rib cage. The visual examinations of predicted rib delineations in a common dataset have demonstrated that the system can achieve a reasonably good performance to be used in practice.

## 1 INTRODUCTION

Diagnostic image analysis is probably the biggest contribution of computer and information sciences to clinical practice in medicine. In the wake of inferring abnormal structures from a medical image without the intervention of a clinician, several attempts have been done to develop intelligent algorithms that can automatically analyze the raw data from various types of modalities. X-ray radiography is known as one of the cheapest and least harmful of these imaging modalities. In spite of the availability of a wide variety of more complicated imaging techniques, it still remains as ubiquitous in medical practice even for well-equipped hospitals and radiology departments. On the other hand, it is also evaluated as most difficult modality to analyze, either manually or computationally, due to the low resolution and high noisy content of the input images.

Chest radiography is one of the most widely used diagnostic tools in x-ray based imaging. A common use is to detect potential lung nodules for the decision of further examination using such as computed tomography or pathology analysis. In addition to major difficulties listed above, chest radiography analysis suffers from normal anatomical structures, such as bones and other overlapping organs, which hide buried abnormalities in normal

tissue of lung. The nodules in the main tissue might be invisible due to the shadows of quasi-parallel bones in the ribcage. Therefore, the delineation and suppression of ribs from the input image without any information loss in the original lung tissue beneath is an important computational challenge in computer-aided diagnosis (CAD) systems for chest radiographs. Whilst this study is motivated from our ultimate goal of suppressing ribs for easier detection of lung nodules, the automatic delineation of ribs has several other benefits, such as providing a frame of reference for locations of abnormalities or detecting rib abnormalities, e.g. fractured or missing ribs. In this study, we address the problem of segmenting the anatomy of ribs in lung images obtained through the x-ray radiography as an intermediate step of rib shadow elimination in CAD systems. To this end, we introduce a novel integrative approach based on parabola curve fitting from rib seeds obtained through a log Gabor filtering. The parabola is extracted from a self-template. The system is completely unsupervised, that is, it does not require any training set of manually delineated ribs or any knowledge-driven rules provided by an expert. The visual examinations of predicted rib delineations in a common dataset have demonstrated that the system can achieve a reasonably good performance to be used in practice.

The automated detection of ribs in chest

radiographs is indeed an old problem in medical image analysis. In one of the earliest studies for rib detection Toriwaki et al. (1980) located rib edges by a template matching approach and fitted parabolas to these borders. This idea later has been used in many studies. De Souza (1983) used the derivatives of vertical profiles to detect the pixels on the rib boundaries and fitted parabola to these. Sarkar et al. (1997) performed a set of gray-level calculation to predict rib border candidates. Yue et al (1995) used a modified Hough transform to fit parabolas to rib edges and refined the boundaries by a snake approach. Vogelsang et al. (1998) followed a similar strategy for fitting parabolas to the edges by a template matching approach and refined the ribs by new estimates of parabolas for each rib. Karargyris et al. (2011) smoothed the detected edges using a Savitzk-Golay filter. Lee et al. (2012) used a knowledge-based generalized Hough transform to locate rib borders starting from a best template detected by a simple Sobel operator. Horvath et al. (2013) refined the final ribs by a dynamic-programming-based active contour algorithm. In general, all methods have three dimensions: detecting the position of upper and/or lower rib borders, fitting a curve to these borders, and refining final rib shadows. It is also worth mentioning about two supervised approaches that used a set of training images with manually delineated rib borders (Ginneken et al, 2000; Loog and Ginneken (2006)) and predicts the locations of ribs from a learned model.

On the contrary to the existing methods that employ a curve fitting from predicted upper or lower rib edges, our system attempts to fit a template of a parabola curve from a seed of rib start point which can be more effectively predicted using a robust log Gabor filtering approach. In this case, a curve somewhere in the middle of the rib can be identified instead of rib borders. Entire rib shadow is delineated by a problem-specific region growing technique, which is also introduced in this paper. This growing stage allows the system to detect exact rib regions which do not necessarily follow the fitted parabola equation extracted from the best template in the same image, which is considered as another major contribution of this study.

The new system is visually examined in a well-known chest radiography set (Shiraishi et al., 2000). It is clearly demonstrated that the rib delineation can be successfully achieved provided that at least one template can be detected from original image. The paper presents the steps of a complete framework starting from several preprocessing stages including

lung segmentation, image enhancement and edge detection and ending with final refinement stages for rib delineation.

## 2 METHODS

### 2.1 Image Preprocessing

In image pre-processing step, we generate Local Contrast Enhanced (LCE) and lung segmented images to be used for template extraction and rib detection steps. The details of these steps are not given in here; a comprehensive description can be found in (Ogul et al., 2015). Template extraction step uses the product of lung segmented LCE and original image as input.

### 2.2 Rib Segmentation

In this section we describe a novel hybrid approach for rib segmentation. The existing systems which model the ribs only using parabola or elliptic equations are lack of the rib shape information because it differs from person to person. We also know that each person have a typical rib shape which do not show significant changes. Therefore, rather than trying to model the ribs regardless of the shape changes, we propose to model the ribs using existing rib templates which are extracted from the overall lung field.

### 2.3 Rib Template Extraction

The rib detection task starts with the extraction of a rib template from the content of query image itself. This allows the framework to exhibit entirely in an unsupervised manner. The template extraction method is inspired from (Lee et al., 2012), where a *locale sampling scheme* technique is first employed to enhance the rib contrast, and then edge detection operator is used to reveal candidate edges, and finally a simple selection scheme is applied to fix the template which appears in the middle of the lung fields. The overall description of their methodology can not detail how to convert edge detected image into binary and how to select the template that appears in the middle of the lung, where both strategy in fact significantly affects the continuity of the rib structure, and in turn the quality of the final rib template extracted. In our study, we get the best binary image results when we use *Minimum Cross Entropy (MCE)* method for thresholding. However, even the best thresholding technique results with

many small non rib candidates and does not provide the rib continuity. Therefore, after *MCE* we apply some morphological operators such as dilation to connect disjointed ribs, opening to remove noise and erosion to construct final rib structure (Fig 1).

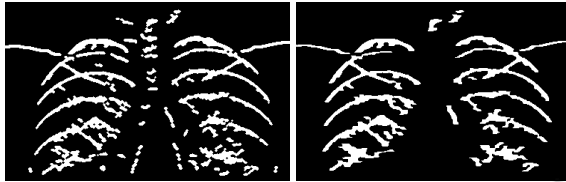


Figure 1: Rib template extraction; first candidates (left), after elimination stage (right).

To select the best candidates, we first flag 8 connected components which have highest pixel count. Then, a thinning morphologic operator takes place. At the final step we remove the templates by their *orientation*, *euler number* and *eccentricity* values. Remaining templates are further reduced after detecting rib starts until we have one template for each of the lung field, which is detailed in following section.

## 2.4 Rib Delineation

The rib delineation through extracted self-templates involves broadly 5 consecutive steps: (i) finding the rib starts at outmost region of ribcage by a log Gabor filtering, (2) selecting a single best template which is most compatible with rib cage, (3) estimating rib thickness, (4) parabola fitting to detect all ribs, and (5) delineating the entire ribs by a specific region growing technique.

### 2.4.1 Finding Outmost Rib Starts

Because the fact that the rib edges are easily affected from high noise levels when pure pixel-based edge detection methods used (Karagyris et al, 2011), we choose to use Log Gabor wavelets in order to find rib borders. Using just the 4<sup>th</sup> scale and the degrees 45° and 135° (Fischer et al., 2009) with Otsu thresholding method gives us not all the rib structures from vertical middle line to the outer borders of the lung but the initial points with real thickness values. In here, initial points refer to the region in which the rib structure intersects with outer border of the lung (Fig 2). Finally, by shifting the lung mask we can see all the ribs positioned on initial points (Fig 2) and we can eliminate the ones which do not appear in initial points. For further steps we also apply thinning morphologic operation so that the ribs are formed as a single-pixel width.

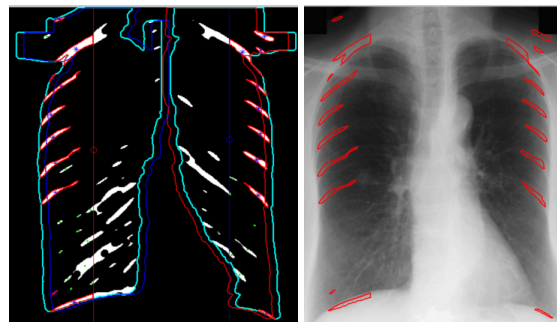


Figure 2: Log Gabor filtering to detect rib seeds.

### 2.4.2 Selecting Best Template

In some cases, the method described in section 2.2.1 gives more than a one template for each of the lung fields while sometimes we just get one template for whole lung region. Thus we need to choose the best template or to form a new one. When the first case occurs, we reduce the templates by calculating their distance to each of the thinned rib structures. The closest template is chosen as the best template. In cases such as a template for a lung field is found, but calculated list for other field is empty, we form the new template by taking the symmetry of existing template.

Calculating the symmetry of a template is not an easy task. It consists of mainly 3 steps: (i) First of all, the best template must be formed as an elliptic curve since it is comprised of scattered pixels (Fig 3, dark blue lines on right lung). Using these non-formed pixels, we find the coefficients for a polynomial  $p(x)$  of degree  $n$  that is a best fit (in a least-squares sense) for the data in  $y$ .

$$p(x) = p_1x^n + p_2x^{n-1} + \dots + p_nx + p_{n+1}$$

(ii) Secondly; its mirror symmetry is calculated (Fig 3, magenta template). (iii) And finally, its final position is found with respect to the center of mass of the region (Fig 3, yellow template). After we compute the  $x$  and  $y$  coordinates of the vertex of the parabola we found in step (i), we can easily calculate the difference between this point and the center of mass of the lung field in which this template lies on. Since this distance should be same on the symmetric lung field, by shifting the symmetric template as the distance value gives us the final template on the left lung in Fig 3 (yellow line).

### 2.4.3 Estimating Rib Thickness

Rib thickness ( $rt$ ) value is used as a stopping criterion while enlarging rib structure from its

center. The main point of calculating  $rt$  is to find the longest vertical line that exists on rib structures. Among all lines we calculate the mean of the values except the ones which are too thin (for JSRT < 10 px.) or thick (>24 px.).

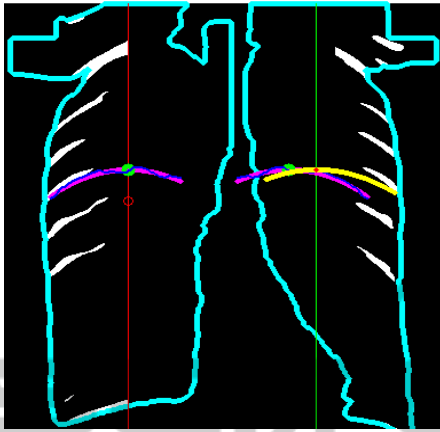


Figure 3: Best template selection step.

#### 2.4.4 Parabola Fitting

Parabola fitting is very important task in which the parameters of the parabola that fits the middle line of each rib structure are calculated. This step is an important basis for region growing and parabola growing algorithms. In subsection 2.2.2.2 we formulated both templates by calculating  $p_1$ ,  $p_2$ ,  $p_3$  values. In order to fit the curve somewhere in the middle of the rib, we need to optimize last parameter of the parabola. While 1<sup>st</sup> and 2<sup>nd</sup> parameters are shape related, 3<sup>rd</sup> parameter has an effect on the position of the template on the rib by moving template up and down. For each rib, keeping first 2 parameters same, we calculated list of  $p_3$  values using each pixel pair that appears in this structure and their mean reports us the final position of the template for its corresponding rib.

#### 2.4.5 Rib Region Growing

Rib delineation is finalized with a two-stage region growing approach. The first stage is the quasi-parallel growing of initial parabola curve fitted to a rib. We use the pixels in the middle of the rib as initial seed points for region growing using 0.015 as threshold value. The grown rib structure has broken pixels on some points. We use these broken pixels for generating our preliminary rib borders. The main idea is repeating to shift the middle-line curve up and down provided that shifted curve contains at least 50% of initially grown pixels.

The first stage of region growing is resulted with a ticker parabola. In some cases we can reach rib borders on region growing part, however mostly the result is thinner structure than actual rib. In the second stage, we consider the rib consists of 4 horizontal parts and use each part individually in order to form them into the final rib structure. For each horizontal part, the growing process is repeated separately on upper or lower part (not on both) based on the mean intensity change until the exact rib with predicted length is formed.

### 3 RESULTS

We compile our method on well-known JSRT dataset having 154 chest x-ray images with known nodules. In 150 of 154 images, at least one template is identified and the best one is selected for self-template matching. In 4 of 154 images, no template is identified. This demonstrates the success of rib template extraction step in general.

In 65% of images, all ribs are perfectly located with a false discovery rate of 8.5%. This detection rate is computed as 90.1% if only one rib is allowed to be missed, which is usually the case since the lowest left rib is often obscured by the heart shadow. Here, we mean by rib detection the correction identification of the position of the rib regardless of that its borders are perfectly located. When each rib is considered as a separate sample, the detection recall (or sensitivity) is 97.1% with a precision of 91.5%. The delineation (locating the exact position of all pixels) performance is not evaluated yet since it requires the contribution of an expert knowledge, which is currently in progress. Nevertheless, we discern the ability of the system to delineate the ribs by a few examples in Figure 4.

### 4 CONCLUSIONS

We introduce a complete framework that takes an unprocessed lung image obtained through a chest radiography and reports the pixels of entire rib regions. The contribution of the study is two-fold. First, a parabola equation extracted from a rib border template is fitted into rib seeds which are defined as the start points of the ribs closer to the outmost (right or left) part of the ribcage. The previous methods largely depend on the quantitative and qualitative value of detected rib borders. Most often, the method employed for edge detection may fail to



cover all ribs in the ribcage or report incorrectly some other curves that resembles a rib boundary. Since the present method does not require the detection of any border but only its outmost starting point, the detection rate can be substantially increased by log Gabor filtering approach. Second contribution is a new region growing technique that is introduced to extend rib center to build the entire rib until rib boundaries are reached. The technique allows each individual rib to grow independently from its initial parabola equation. In that sense, the difference between the curvative structure of upper and lower ribs can be elaborated. Based on the visual examinations of a common dataset of lung images, we can argue that the results are very promising to continue with a suppression method that follows the rib delineation.

The future work will involve: (1) a quantitative evaluation the results after a manual delineation of rib borders by an observer, (2) a qualitative evaluation of the results by a committee of radiology experts, (3) improving the algorithm that smoothes the rib boundaries by a dynamic programming approach, and finally (4) applying a data-driven bone suppression technique to make the main tissue more visible so that the abnormalities beneath the ribs can be easily identified.

## ACKNOWLEDGEMENTS

This study was supported by Turkey Ministry of Science, Technology and Industry by the grant number 379.STZ.2013-2, and Akgun Software Company.

## REFERENCES

- De Souza P., Automatic rib detection in chest radiographs, *Comput. Vis., Graphics, Image Process.*, vol. 23, pp.129-161, 1983.
- Fischer, S., Redondo, R. and Cristobal, G. "How to construct Log-Gabor filters", Open Access Digital CSIC Document, 2009.
- Horváth A., Orbán G.G., Horváth A., Horváth G., An X-ray CAD system with ribcage suppression for improved detection of lung lesions, *Periodica Polytechnica Electrical Engineering and Computer Science*, vol. 57, pp. 19-33, 2013.
- Karagyris, A., Antani, S., Thoma, G., Segmenting anatomy in chest x-rays for tuberculosis screening, *Engineering in Medicine and Biology Society, EMBC, 2011 Annual International Conference of the IEEE*, On page(s): 7779 - 7782.
- Lee J.S., Wang J.W., Wuc H.H., Yuand M.Z., A nonparametric-based rib suppression method for chest radiographs *Computers & Mathematics with Applications*, Volume 64, Issue 5, September 2012, Pages 1390–1399.
- Loog, M.; Ginneken, B. "Segmentation of the posterior ribs in chest radiographs using iterated contextual pixel classification", *Medical Imaging, IEEE Transactions on*, On page(s): 602 - 611 Volume: 25, Issue: 5, May 2006.
- Ogul B.B., Kosucu P., Özcamlar A., Kanik S.D, Lung Nodule Detection in X-Ray Images: A New Feature Set, 6th European Conference of the International Federation for Medical and Biological Engineering, *IFMBE Proceedings Volume 45*, 2015, pp 150-155.
- Sarkar S. and Chaudhuri S., Detection of rib shadows in digital chest radiographs, *Proc. ICIAP (2)*, pp.356 - 363 1997.
- Shiraishi J, Katsuragawa S, Ikezoe J, Matsumoto T, Kobayashi T, Komatsu K, Matsui M, Fujita H, Kodera Y, and Doi K.: Development of a digital image database for chest radiographs with and without a lung nodule: Receiver operating characteristic analysis of radiologists detection of pulmonary nodules. *AJR* 174; 71-74, 2000.
- Toriwaki J., Hasegawa J, Fukumura T, Tagaki Y, (1980), Computer analysis of chest photofluorograms and its application to automated screening, *Automedica* 3, 63-81.
- van Ginneken B. and ter Haar Romeny V, Loew M. H. and Sonka M., Automatic delineation of ribs in frontal chest radiographs, *Image Process.*, vol. 3979, pp.825-836 2000.
- Vogelsang F., Weiler F., Dahmen J., Kilbinger M.W., Wein B.B., Guenther R.W., Detection and compensation of rib structures in chest radiographs for diagnostic assistance, *SPIE Proceedings Vol.3338: Medical Imaging 1998: Image Processing*.
- Yue Z., Goshtasby A. and Ackerman L. V., Automatic detection of rib borders in chest radiographs, *IEEE Trans. Med. Imag.*, vol. 14, no. 3, pp.525-536 1995.

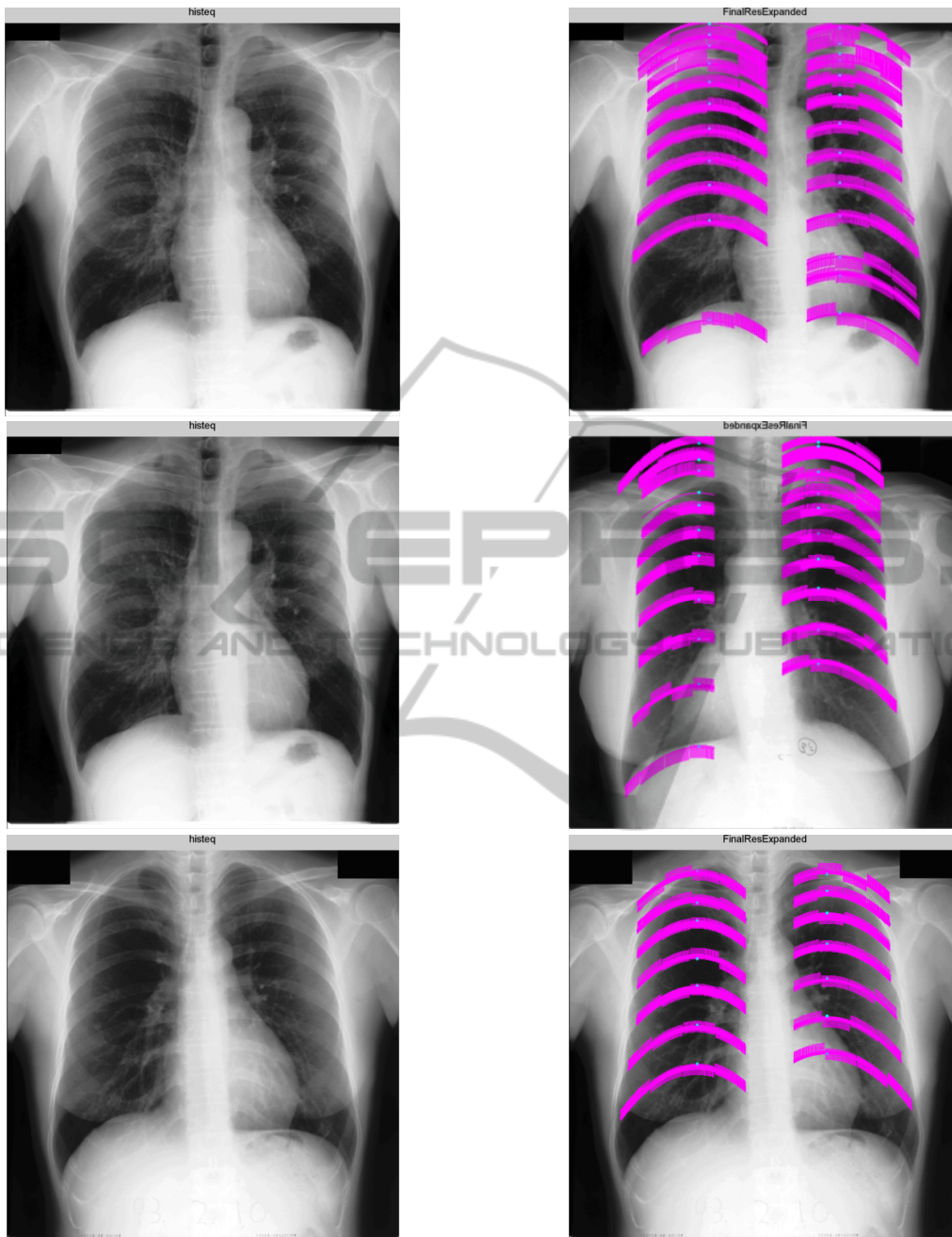


Figure 4: Example chest radiography images (left) and delineated ribs by our system (right).